Tangled up in fibers: How a lytic polysaccharide monooxygenase binds its chitin substrate

Henrik Vinther Sørensen[1,§], Mateu Montserrat-Canals[1,2], Sylvain Prévost[3], Gustav Vaaje-Kolstad[4], Kaare Bjerregaard-Andersen[1,§], Reidar Lund[1*], Ute Krengel[1*]

[1] Department of Chemistry, University of Oslo, NO-0315 Oslo, Norway

[2] Centre for Molecular Medicine Norway, University of Oslo, NO-0318 Oslo, Norway

[3] Large-Scale Structures group, Institut Laue-Langevin, 71 avenue des Martyrs, 38042 Grenoble, France

[4] Faculty of Chemistry, Biotechnology and Food Science, Norwegian University of Life Sciences (NMBU), NO-1340 Ås, Norway

[§] Present addresses: Henrik V. Sørensen, Division of Computational Chemistry, Lund University, SE-223 62, Sweden; Kaare Bjerregaard-Andersen, Ottilia vej 9, H. Lundbeck A/S, DK-2500 Valby, Denmark

*Correspondence: Reidar Lund (reidar.lund@kjemi.uio.no); Ute Krengel (ute.krengel@kjemi.uio.no)

Abstract

Lytic polysaccharide monooxygenases (LPMOs) are redox-enzymes that bind to and oxidize insoluble carbohydrate substrates, such as chitin or cellulose. This class of enzymes has attracted considerable attention due to their ability to convert biomaterials of high abundance into oligosaccharides that can be useful for producing biofuels and bioplastics. However, processes at the interface between solution and insoluble substrates represent a major challenge to biochemical and structural characterization. This study used the four-domain LPMO from *Vibrio cholerae*, *N*-acetyl glucosamine binding protein A (GbpA), to elucidate how it docks onto its insoluble substrate with its two terminal domains. First, we developed a protocol that allowed GbpA and chitin to form a stable complex in suspension, overcoming incompatibilities of the two binding partners with respect to pH. After determining the neutron scattering contrast match point for chitin, we characterized the structure of GbpA in complex with chitin by Small-Angle Neutron Scattering (SANS). We found that GbpA binds rapidly to chitin, where it spreads out on the chitin fibers unevenly. These findings are supported by electron microscopy. Placing our findings into a biological context, we discussed the potential advantages of GbpA secretion and how chitin binding may prepare the ground for microcolony formation of the bacteria.

Keywords: GbpA: LPMO; chitin complex; secreted colonization factor; contrast matching; Small-Angle Neutron Scattering; Bio-SANS; *Vibrio cholerae*

1. Introduction

Since the discovery of lytic polysaccharide monooxygenases (LPMOs) in 2010 [1], their ability to degrade crystalline cellulose, xylan or chitin has drawn massive interest for conversion of renewable biomaterials to biofuels. LPMOs are multi-domain proteins found in a wide range of organisms, including bacteria, fungi, algae and insects, as well as viruses [2, 3]. The proteins are secreted by human pathogenic bacteria and employed for survival both outside the host on carbohydrate surfaces, and inside the host, using different strategies [4-6], including direct interference with the immune system [6]. Given the abundance of these enzymes, and their sequence variation, it is likely that other important functions of these proteins are yet to be revealed. The discovery of LPMOs necessitated a reclassification of enzyme families in the Carbohydrate-Active enZYmes database (CAZY; http://www.cazy.org), where they are listed under 'auxiliary activities' families (AA9-11 and AA13-17). The first crystal structures of LPMO complexes with carbohydrate ligands (cellotriaose, Glc_3 and cellohexaose, Glc_6) were solved in 2016 by Frandsen *et al.* [7], for an AA9 LPMO from *Lentinus similis*. At approximately the same time, Courtade *et al.* probed ligand binding to another AA9 LPMO, from *Neurospora crassa*, by nuclear magnetic resonance (NMR) spectroscopy [8]. These and subsequent studies showed how the ligand stretches across the flat surface of the pyramidal LPMO structure, with the +1 sugar unit binding to the N-terminal histidine of the characteristic copper-coordinating histidine-brace-motif in the active site of LPMOs. The catalytic mechanism of LPMOs, and current controversies, are summarized in an excellent review by Forsberg *et al.* [9]. Despite increasing structural and functional data, there is scarce structural information on the molecular interaction of LPMOs with their complex recalcitrant carbohydrate substrates.

We are interested in virulence factors of *Vibrio cholerae,* the causative agent of cholera. Therefore we selected *N*-acetylglucosamine binding protein A (GbpA) from *Vibrio cholerae*, as a model system to study its interaction with chitin (for a review of chitin-active LPMOs, see Courtade & Aachmann [3]). GbpA was discovered in 2005 [4], and found to be important for colonization in the aquatic environment [4, 10, 11] as well as the human host, binding to (and up-regulating) human mucins [5, 10]. GbpA consists of four domains, of which the first domain, which structurally resembles carbohydrate-binding module CBM33, is a chitin-degrading LPMO [12, 13] and additionally binds to mucins [12]. The fourth domain (classified as a CBM73 in CAZy) also binds chitin [12], whereas domains 2 and 3, which structurally resemble flagellin and pilin-binding proteins, respectively, mediate attachment to the cell surface of the bacteria [12]. The structure of the first three domains of GbpA has been solved by X-ray crystallography [12], recently complemented with the full-length crystal structure of a GbpA homolog from *Vibrio campbellii* [14]. In addition, the solution structure of GbpA has been characterized with Small-Angle X-ray Scattering (SAXS) and Small-Angle X-ray Scattering (SANS) [12, 15], revealing a monomeric elongated structure. How the structure of GbpA changes upon binding to chitin, and how the domains align in this state, is, however, unknown.

Here, we set out to reveal how GbpA interacts with chitin fibers with Small-Angle Neutron Scattering (SANS). We characterized the bound and unbound GbpA structures by applying

SANS to deuterated and non-deuterated GbpA (alone or in complex with chitin), and by varying the contrast with D_2O/H_2O-mixtures, as schematically shown in Figure 1. Additional, complementary insights were obtained from negative-stain electron microscopy (EM).

2. Materials and methods

2.1 Protein production and deuteration

Perdeuteration of GbpA involved expression in deuterated media, according to the protocol described in [15], which was inspired by [16]. This protocol relies on BL21 star (DE3) cells containing the GbpA-encoding gene in the pET22b vector [15]. Growth and expression media contained D_2O and d_8-glycerol (99% D) purchased from ChemSupport AS (Hommelvik, Norway). The production of H-GbpA and the purification of D-GbpA and H-GbpA is also described in [15].

GbpA was saturated with copper to activate the enzyme prior to the SANS experiments, by incubation with $CuCl_2$ in 5-fold molar excess for at least 30 min. Free copper was then removed by passing the protein through a HiTrap Desalting column (GE Healthcare). Prior to the SANS experiments, the protein was dialyzed against 100 mM NaCl, 20 mM Tris-HCl pH 8.0 with 47% of the water being D_2O.

2.2 Preparation of chitin, GbpA and chitin-GbpA samples for SANS

β-chitin nanofibers (≈180 micrometer in length) from squid pens (France Chitine, Orange, France) were kindly provided by Jennifer Loose and Gustav Vaaje-Kolstad and prepared according to the protocol described in [13]. The fibers were dissolved in 20 mM acetic acid (pH 3.2) to a concentration of 10 mg/mL and subsequently sonicated at 50-70% power with a Vibra Cell Ultrasonic Processor until they were well dispersed and did not sink to the bottom of the tube for days. Finally, the fiber suspension was dialyzed against 20 mM sodium acetate-HAc pH 5.0 with the desired amount of D_2O for at least 24 hours. At higher pH or in the presence of salts, it was observed that the fibers precipitated. However, at pH 5, GbpA is not very stable. Nevertheless, it was possible to add GbpA to the fibers from a highly concentrated stock solution of the protein (prepared by dialysis against 10 mM NaCl, 20 mM Tris-HCl pH 8.0), if the mixture was immediately treated by thorough pipetting (*i.e.*, pipetting the suspension up and down 7-10 times with a micro pipette, using a cut-off 1 mL pipette tip). We observed that the mixture became less viscous in this process. To further stabilize the suspension, we sonicated the mixture for 15-30 sec with a tip sonicator and re-dialyzed the sample for 24 hours against 20 mM sodium acetate-HAc pH 5.0 with relevant amounts of D_2O. After any dilution of the chitin fibers or the mixture, the solutions were re-sonicated for 15-30 seconds to ensure proper suspension.

GbpA samples without chitin were dialyzed into 100 mM NaCl, 20 mM Tris-HCl pH 8.0, with the desired level of D_2O prior to SANS analysis.

2.3 SANS measurements

Samples were measured with Small-Angle Neutron Scattering (SANS) at beamline D11 at Institut Laue-Langevin (ILL) [17], with wavelength $\lambda = 5.6$ Å and a wavelength spread of $\Delta\lambda/\lambda = 9\%$. Data were acquired for the q-range of 0.0013 – 0.4102 $Å^{-1}$. Ultra Small-Angle Neutron Scattering (USANS) experiments were carried out at beamline BT5 [18] at the National Institute of Standards and Technology (NIST) Center for Neutron Research, using $\lambda = 2.4$ Å and a wavelength spread of 6% $\Delta\lambda/\lambda$, for the q-range 0.00005 $Å^{-1}$ to 0.001 $Å^{-1}$.

Tumbling cells were used for USANS measurements. To find the chitin match point, 10 mg/mL chitin was measured in 0%, 20%, 42%, 66%, 80% and 100% D_2O for 15 min per sample at ILL beamline D11. The data were integrated from 0.03 to 0.4 $Å^{-1}$, and the integrated data were fitted with a second degree polynomial function. The chitin match point was estimated from the minimum of this function.

While SANS samples were measured for 2-3 hours, USANS measurements lasted 11 hours per sample. Buffer, empty cell and H_2O measurements were used for background subtraction and calibration to absolute scale. Processing was done with software at the respective beamlines [19, 20]. Low-q data ($q < 0.004$ $Å^{-1}$) were fitted with a power law model:

(1) $I(q) = Bq^{-D}$

where B is a scaling factor, and D the decay exponent related to the apparent fractal dimension, if $1 < D < 3$ or surface scattering if $D = 4$. Data plotting and modeling were performed with Origin (Version 2017 64bit, OriginLab Corporation) and QtiSAS [21].

2.4 Negative-stain EM

GbpA and chitin samples were prepared, essentially as described above. 10 mL of 3 mg/mL chitin were subjected to sonication in 20 mM acetic acid pH 3.2. Sonication was performed in a Q500 Sonicator (Qsonica), using the thinnest tip at 30% intensity in 3/3 sec on/off pulses until the sample was completely suspended. Chitin was dialyzed overnight against 20 mM acetic acid pH 5.0 and sonicated again to ensure that it remained suspended. A few microliters of concentrated GbpA in 20 mM Tris-HCl pH 8.0 and 50 mM NaCl were added to 200 μL of the chitin suspension to a final concentration of 2 mg/mL of GbpA, and mixed thoroughly with the use of a pipette. Staining and imaging were performed immediately thereafter (without re-sonication) to prevent chitin precipitation.

Samples were applied to carbon-coated 300 mesh Cu TEM grids and blotted. Immediately thereafter, they were washed twice in water and stained with uranyl acetate 1% for a few seconds. Images were acquired with a JEM-1400Plus microscope operating at 120kV, and processed with ImageJ [22].

3. Results and Discussion

3.1 Development of a protocol for solution studies

A suitable method for structural characterization of individual partners in a protein complex is SANS, in combination with SAXS. Both are solution techniques. This poses a challenge for studying protein complexes of chitin, which is an insoluble homopolymer of *N*-acetyl glucosamine (GlcNAc) residues. To our knowledge, chitin has rarely been used for solution scattering studies, because of its low solubility. It has, however, been shown that fine β-chitin nanofibers can be suspended in slightly acidic buffers (pH∼3) [13, 23]. For shorter periods of time, chitin can be kept at pH∼5, however, this is still low for GbpA, which shows some precipitation at pH ≤ 5. Fortunately, we could overcome these challenges by adding small volumes of 10-12 mg/mL GbpA (pH = 8.0) to chitin nanofibers (pH = 5.0), followed by immediate thorough pipetting and —for SAXS and SANS experiments— sonication for 15-20 sec with a tip sonicator, as described in *Section* 2.2. The such-treated samples were subsequently dialyzed to 20 mM sodium acetate-HAc pH∼5 during a 24-hour period. After this procedure, the chitin-GbpA complex could be kept in suspension for 12-24 hours, sufficient for several SANS experiments. For the lengthier USANS measurements, rotating tumbler cells were used to keep the samples in suspension. In case of delays, it is recommended that the complex is re-sonicated directly before the experiments. We observed that solubility of the chitin fibers increases after addition of GbpA, indicating that a complex has indeed formed. It was even possible to adjust the pH of the complex mixture to higher pH values (∼7), without immediate precipitation.

3.2 Chitin can be matched out in SANS

To obtain structural information of GbpA in its chitin-bound state with SANS, it is necessary to measure the sample at the chitin D_2O/H_2O match point. Since this match point has not previously been established, we set out to do so. After dispersing the fibers evenly in 20 mM acetic acid (pH 3.2), the suspension was dialyzed into six different levels of D_2O and measured by SANS (Figure 2A). We calculated the chitin match point to be at 47% D_2O (Figure 2B). This is extremely close to the theoretical match point of most globular proteins (≈40-45% D_2O), necessitating the use of deuterated GbpA (D-GbpA) for SANS interaction studies since it has a significantly different match point (> 100% D_2O). To confirm that chitin is well matched out in the q-range where D-GbpA scatters and show that D-GbpA can indeed be used for interaction studies with chitin at the match point, we measured chitin, D-GbpA and non-deuterated GbpA (H-GbpA) individually at 47% D_2O (Figure 2C-D). The scattering of 50 µM (2.5 mg/mL) D-GbpA at 47% was much stronger than for chitin, which was well matched out, except at very low q-values, giving us green light regarding the feasibility of the planned SANS experiments with D-GbpA. The results also suggested that using H-GbpA would be impossible for this kind of study, as it scatters poorly at 47% D_2O.

3.3 GbpA decorates chitin fibers

Based on the promising initial experiments regarding contrast matching of chitin, we progressed to study the complex of chitin and GbpA. An indication of complex formation was already obtained upon mixture of the two components, as described above. The chitin

suspension is highly viscous, but upon addition of D-GbpA and sonication, the solution became easier to pipet and less sticky to surfaces (images of the chitin solution and the mixture are shown in Figure 3A, B). The SANS curve of the complex at the chitin match point (Figure 3C, D) lacked the features of GbpA at high q-values, indicating a preference for the chitin-bound state and a conformational change of GbpA. Interestingly, the SANS curve was similar to the SANS curve of chitin itself, at a good contrast (100% D_2O); in particular, a steep slope at low q-values was present for both chitin and the complex mixture (Figure 3E). This strongly indicates that GbpA binds along the chitin fibers. It also indicates that chitin-bound GbpA does not scatter as independent particles, but that there is structural correlation between the protein molecules. Unfortunately, this made it impossible to obtain a structural model of GbpA in the chitin-bound conformation.

We fitted the low-q region of chitin and the chitin-GbpA data with a power law with the decay exponent *D* and *B* as a scaling factor (results are summarized in Table 1). The decay exponent describes the fractal dimensionality of the aggregate or surface scattering (Porod-like) if $D \sim 4$ [24]. Chitin itself has a decay exponent of 4.3, indicating very large aggregates, with a sharply defined surface [24, 25]. For the GbpA-chitin complex at the chitin match point, the decay exponent is 2.7, indicating aggregates in a state between random and globular.

In an attempt to reveal the scattering of individual GbpA particles on the chitin fibers, we decreased the crowding on the fibers by using a higher ratio of chitin to GbpA (Figure 3E), but this did not change the slope at low-q significantly. The decay exponent was 3.0, indicating an open, globular aggregate. At mid-q values, we could, however, observe a significant difference in intensity (bump indicated by red arrow in Figure 3E), possibly due to a change in the thickness of the fibers from the decoration of chitin with GbpA. This indicates possible crowding of GbpA on the chitin fibers, which may also involve protein-protein interactions.

These results were visually confirmed in the EM micrographs shown in Figures 4 and 5, where chitin fibers appear more electron-dense and thicker when coated with GbpA (17.7 nm vs 7.5 nm in average). The uniform increase in thickness along individual chitin fibers suggests that GbpA completely covers chitin. GbpA measures approximately 5 nm on the axis perpendicular to the chitin fibers, which suggests that GbpA binds to chitin in an extended conformation, with the two chitin-binding domains facing in the same direction, as depicted in Figure 1. A difference in fiber thickness of 10.2 nm with or without GbpA (corresponding to two GbpA molecules in a 2D projection) suggests coating of the chitin fibers with a single layer of GbpA molecules around the longitudinal fiber axis.

3.4 GbpA does not cover chitin uniformly

If GbpA does not bind evenly to the chitin fibers, as originally anticipated, but instead forms clusters of multiple protein molecules, our attempt to increase the ratio of chitin to GbpA in order to spread out the GbpA molecules would not work. To address this problem in a different way, we used mixtures of H-GbpA and D-GbpA bound to chitin at the chitin match point (Figure 3F). Since H-GbpA is well matched out at the chitin match point of 47% D_2O, we expected to still mostly see D-GbpA on the chitin fibers. However, since D-GbpA and H-GbpA compete for the binding sites, the distance between D-GbpA on the fibers should increase,

perhaps to the point of scattering independently. As expected, the SANS intensities for the mixtures of D-GbpA and H-GbpA on chitin decreased with higher proportion of H-GbpA (Figure 3F). However, the slope at low q did not decrease. This showed that even when the distance between D-GbpA particles on chitin is increased, D-GbpA molecules did not scatter independently. When only using H-GbpA, the slope at low q was like that of chitin alone (Table 1). This was not unexpected, since H-GbpA is better matched out in this q-range than chitin, therefore the slope at low-q will be dominated by the chitin aggregates. However, for D-GbpA, the slope at low q is different to that of chitin alone, indicating a different fractal dimension. This could in principle have two different explanations: (a) either GbpA binding affects the chitin structure, or (b) GbpA binds unevenly to the chitin fibers. Given that the SANS curve for the H-GbpA–chitin complex has a similar slope as chitin alone, we can exclude (a). The lower decay exponent of D-GbpA in the chitin-bound state, compared to the decay exponent of chitin, can therefore only be explained by GbpA binding unevenly on the chitin fibers, with a preference for certain parts of the network. This is also consistent with SANS measurements of the D-GbpA–chitin complex at D_2O levels between the match points of the two components (Figure 3G), where the decay exponent was calculated to be 3.4.

We performed Ultra-Small-Angle Neutron Scattering (USANS) experiments, which give structural information in the hundreds of nanometer range, thus providing an estimate of the size of aggregates. However, we observed that the slope for the chitin-bound GbpA extends to very low angles, without flattening out, indicating that GbpA decorates very large areas, or domains, on the chitin fibers (Figure 6). It is not trivial to conclude exactly how GbpA binds to these areas, if it for example forms multiple local clusters or if the molecules spread out evenly within the confines of these domains. However, EM analysis provided a good explanation of the results observed with SANS and USANS, with GbpA inducing aggregation of chitin fibers and creating fiber clumps as observed in Figure 4 (panels C, D and F).

3.5 Discussion of experiments

It may not be possible to obtain a structural model of independently scattering GbpA particles on β-chitin fibers using SANS, due to persisting structural order along the chitin fibers. This is not surprising, since the fibers are long, and likely rigid, inducing a fixed order even over long distances. Much shorter chitin fibers would be required in order to overcome these technical impediments. However, we have obtained other important insights: our study demonstrates that it is possible to use chitin in neutron scattering studies, as the polymer can be well matched out in the mid to high-q range at 47% D_2O. Using both SANS and EM, we could further show that GbpA decorates the chitin fibers with many binding sites over the chitin network, and with a preference for the chitin-bound state over the solution state. This explains why GbpA can effectively degrade insoluble chitin substrates, while glycosidic hydrolases cannot. GbpA does not adsorb evenly to all parts of the chitin network, possibly because some parts of the fibers are less accessible than others. The regions of chitin with high accessibility for GbpA binding likely exhibit protein-protein interactions yet to be elucidated. We observed that upon GbpA-binding to chitin, the suspension of chitin fibers immediately becomes less viscous, suggesting that the properties of the GbpA-chitin complex

differ significantly from those of both partners alone. However, the overall structure of chitin remains otherwise unchanged.

The results presented here will be useful to guide future studies, potentially involving other methods, such as neutron reflectometry on flat surfaces of chitin, or cryo–electron tomography.

3.6 Implications for GbpA's role as colonization factor

Chitin is the most abundant biopolymer in marine environments, and is found *e.g.*, on zooplankton, mussels and crustaceans. *V. cholerae* would therefore be well served by using a chitin-binding colonization factor, *i.e.* GbpA, as one of its first anchors when forming microcolonies (as suggested by [26]). Other important factors for microcolony formation are the toxin-co-regulated pilus (TCP) [27, 28], the chitin regulated pilus (ChiRP) [29] and outer membrane adhesion factor multivalent adhesion molecule 7 (Mam7) [30]. An extracellular matrix consisting of polysaccharides and proteins then encases the microcolonies, completing the protected environment by forming a biofilm [31-34], which can adapt to changing environmental conditions [35, 36] and raises infectivity [37]. Chitin binding may thus initiate a cascade of events that culminates in biofilm formation and hyper-infectivity. Moreover, chitin binding has been shown to induce natural competence in *V. cholerae* [38], increasing bacterial fitness by exchange of genes. The first step of these events appears to be the secretion of GbpA and chitin binding. – But why would it make sense for the bacteria to throw out anchors without a connecting line, and attaching to them in a second step? The picture emerging from the present study is that GbpA efficiently prepares the ground for microcolony formation by forming aggregates dispersed throughout the fibers, and with this reserves space for *V. cholerae* over competitors, as previously suggested by Kirn *et al.* [4]. Secreting anchors first, and then attaching to them, and reproducing, allows the bacteria to most effectively colonize biotic surfaces in the aquatic environment. Additionally – and at least as important –, GbpA ensures abundant food supplies through its lytic polysaccharide mono- (or per-) oxidase activity, giving the bacteria an excellent return on their initial energy investment when producing and secreting GbpA.

Acknowledgements

We thank Jennifer Loose for a very nice collaboration on the GbpA project. We further wish to thank the staff at NIST (Susan Krueger, Markus Bleuel, Paul Butler and Susana M. Teixeira) for outstanding beamline support and very fruitful discussions, and Mark Bleuel and Susan Krueger for preliminary comments on this manuscript. We are grateful to Norbert Roos for EM grid preparation and image acquisition at the UiO core facilities of the Life Science Electron Microscopy Consortium (LSEMC). Other work at UiO was performed at the UiO Structural Biology core facilities, belonging to NORCRYST, and at RECX, two national Norwegian core facilities. Work at international facilities was supported through granting research proposals no. 8-03-988 (ILL), no. 1920565 (ISIS) and no. 27117 (NIST). We are pleased to acknowledge funding by the Norwegian Research Council (grant no. 272201). Access to the USANS instrument was provided by the Center for High Resolution Neutron Scattering, a partnership between the National Institute of Standards and Technology and the National Science Foundation under Agreement No. DMR-2010792.

National Institute of Standards and Technology disclaimer

Certain commercial equipment, instruments, materials, suppliers, or software are identified in this paper to foster understanding. Such identification does not imply recommendation or endorsement by the National Institute of Standards and Technology (NIST) nor does it imply that the materials or equipment identified are necessarily the best available for the purpose.

Author contributions

K.B.-A. and U.K. conceived the study. H.V.S. and M.M.-C. produced the protein, and H.V.S. established a protocol for sample preparation and performed SANS experiments, supervised by K.B.-A., R.L. and U.K., and with assistance of S.P. at ILL. M.M.-C. prepared the samples for EM and acquired the data at the EM core facilities at UiO. G.V.-K. supported the work with samples and know-how. The manuscript was written by H.V.S., with contributions from M.M.-C. and U.K.. It was revised with input and approval from all authors.

References

1. Vaaje-Kolstad, G., Westereng, B., Horn, S.J., Liu, Z., Zhai, H., Sørlie, M., and Eijsink, V.G.H. (2010). An oxidative enzyme boosting the enzymatic conversion of recalcitrant polysaccharides. Science *330*, 219-222.
2. Vaaje-Kolstad, G., Forsberg, Z., Loose, J.S.M., Bissaro, B., and Eijsink, V.G.H. (2017). Structural diversity of lytic polysaccharide monooxygenases. Curr. Opin. Struct. Biol. *44*, 67-76.
3. Courtade, G., and Aachmann, F.L. (2019). Chitin-active lytic polysaccharide monooxygenases. Advances in Experimental Medicine and Biology *1142*, 115-129.
4. Kirn, T.J., Jude, B.A., and Taylor, R.K. (2005). A colonization factor links *Vibrio cholerae* environmental survival and human infection. Nature *438*, 863-866.
5. Bhowmick, R., Ghosal, A., Das, B., Koley, H., Saha, D.R., Ganguly, S., Nandy, R.K., Bhadra, R.K., and Chatterjee, N.S. (2008). Intestinal adherence of *Vibrio cholerae* involves a coordinated interaction between colonization factor GbpA and mucin. Infect. Immun. *76*, 4968-4977.
6. Askarian, F., Uchiyama, S., Masson, H., Sørensen, H.V., Golten, O., Bunæs, A.C., Mekasha, S., Røhr, Å.K., Kommedal, E., Ludviksen, J.A., et al. (2021). The lytic polysaccharide monooxygenase CbpD promotes *Pseudomonas aeruginosa* virulence in systemic infection. Nat. Commun. *12*.
7. Frandsen, K.E.H., Simmons, T.J., Dupree, P., Poulsen, J.-C.N., Hemsworth, G.R., Ciano, L., Johnston, E.M., Tovborg, M., Johansen, K.S., von Freiesleben, P., et al. (2016). The molecular basis of polysaccharide cleavage by lytic polysaccharide monooxygenases. Nat. Chem. Biol. *12*, 298-303.
8. Courtade, G., Wimmer, R., Røhr, Å.K., Preims, M., Felice, A.K.G., Dimarogona, M., Vaaje-Kolstad, G., Sørlie, M., Sandgren, M., Ludwig, R., et al. (2016). Interactions of a fungal lytic polysaccharide monooxygenase with β-glucan substrates and cellobiose dehydrogenase. PNAS *113*, 5922-5927.
9. Forsberg, Z., Sørlie, M., Petrović, D., Courtade, G., Aachmann, F.L., Vaaje-Kolstad, G., Bissaro, B., Røhr, Å.K., and Eijsink, V.G.H. (2019). Polysaccharide degradation by lytic polysaccharide monooxygenases. Curr. Opin. Struct. Biol. *59*, 54-64.
10. Zampini, M., Pruzzo, C., Bondre, V.P., Tarsi, R., Cosmo, M., Bacciaglia, A., Chhabra, A., Srivastava, R., and Srivastava, B.S. (2005). *Vibrio cholerae* persistence in aquatic environments and colonization of intestinal cells: involvement of a common adhesion mechanism. FEMS Microbiol. Lett. *244*, 267-273.
11. Stauder, M., Huq, A., Pezzati, E., Grim, C.J., Ramoino, P., Pane, L., Colwell, R.R., Pruzzo, C., and Vezzulli, L. (2012). Role of GbpA protein, an important virulence-related colonization factor, for *Vibrio cholerae*'s survival in the aquatic environment. Environ. Microbiol. Rep. *4*, 439-445.
12. Wong, E., Vaaje-Kolstad, G., Ghosh, A., Hurtado-Guerrero, R., Konarev, P.V., Ibrahim, A.F.M., Svergun, D.I., Eijsink, V.G.H., Chatterjee, N.S., and van Aalten, D.M.F. (2012). The *Vibrio cholerae* colonization factor GbpA possesses a modular structure that governs binding to different host surfaces. PLoS Pathog. *8*, e1002373.
13. Loose, J.S.M., Forsberg, Z., Fraaije, M.W., Eijsink, V.G.H., and Vaaje-Kolstad, G. (2014). A rapid quantitative activity assay shows that the *Vibrio cholerae* colonization factor GbpA is an active lytic polysaccharide monooxygenase. FEBS Lett. *588*, 3435-3440.
14. Zhou, Y., Wannapaiboon, S., Prongjit, M., Pornsuwan, S., Sucharitakul, J., Kamonsutthipaijit, N., Robinson, R.C., and Suginta, W. (2023). Structural and binding studies of a new chitin-active AA10 lytic polysaccharide monooxygenase from the marine bacterium *Vibrio campbellii*. Acta Crystallogr. D: Struct. Biol. *79*, 479-497.
15. Sørensen, H.V., Montserrat-Canals, M., Loose, J., Fisher, Z., Moulin, M., Blakeley, M., Cordara, G., Bjerregaard-Andersen, K., Krengel, U. (2023). Perdeuterated GbpA enables neutron scattering experiments of a lytic polysaccharide monooxygenase. ACS Omega *8*, 29101-29112
16. Cai, M., Huang, Y., Yang, R., Craigie, R., and Clore, G.M. (2016). A simple and robust protocol for high-yield expression of perdeuterated proteins in *Escherichia coli* grown in shaker flasks. J. Biomol. NMR *66*, 85-91.
17. Lindner, P., and Schweins, R. (2010). The D11 small-angle scattering instrument: a new benchmark for SANS. Neutron News *21*, 15-18.

18. Barker, J.G., Glinka, C.J., Moyer, J.J., Kim, M.H., Drews, A.R., and Agamalian, M. (2005). Design and performance of a thermal-neutron double-crystal diffractometer for USANS at NIST. J. Appl. Crystallogr. *38*, 1004-1011.

19. Richard, D., Ferrand, M., and Kearley, G.J. (1996). Analysis and visualisation of neutron-scattering data. J. Neutron Res. *4*, 33-39.

20. Kline, S.R. (2006). Reduction and analysis of SANS and USANS data using IGOR Pro. J. Appl. Crystallogr. *39*, 895-900.

21. Pipich, V. (2020). QtiSAS: user-friendly program for reduction, visualization, analysis and fit of SA(N)S data. URL: http://www.qtisas.com (Accessed 03.2021).

22. Schneider, C.A., Rasband, W.S., Eliceiri, K.W. (2012). NIH Image to ImageJ: 25 years of image analysis. Nat. Methods *9*, 671-675.

23. Fan, Y., Saito, T., and Isogai, A. (2008). Preparation of chitin nanofibers from squid pen β-chitin by simple mechanical treatment under acid conditions. Biomacromolecules *9*, 1919-1923.

24. Larsen, A.H., Pedersen, J.S., and Arleth, L. (2020). Assessment of structure factors for analysis of small-angle scattering data from desired or undesired aggregates. J. Appl. Crystallogr. *53*, 991-1005.

25. Pedersen, J.S. (1993). Small-angle scattering from precipitates: Analysis by use of a polydisperse hard-sphere model. Phys. Rev. B Condens Matter *47*, 657-665.

26. Almagro-Moreno, S., Pruss, K., and Taylor, R.K. (2015). Intestinal colonization dynamics of *Vibrio cholerae*. PLOS Pathog. *11*, e1004787.

27. Taylor, R.K., Miller, V.L., Furlong, D.B., and Mekalanos, J.J. (1987). Use of *phoA* gene fusions to identify a pilus colonization factor coordinately regulated with cholera toxin. Proc. Natl. Acad. Sci. U.S.A. *84*, 2833-2837.

28. Voss, E., and Attridge, S.R. (1993). *In vitro* production of toxin-coregulated pili by *Vibrio cholerae* El Tor. Microb. Pathog. *15*, 255-268.

29. Meibom, K.L., Li, X.B., Nielsen, A.T., Wu, C.Y., Roseman, S., and Schoolnik, G.K. (2004). The *Vibrio cholerae* chitin utilization program. Proc. Natl. Acad. Sci. U.S.A. *101*, 2524-2529.

30. Krachler, A.M., Ham, H., and Orth, K. (2011). Outer membrane adhesion factor multivalent adhesion molecule 7 initiates host cell binding during infection by Gram-negative pathogens. Proc. Natl. Acad. Sci. U.S.A. *108*, 11614-11619.

31. Watnick, P.I., and Kolter, R. (1999). Steps in the development of a *Vibrio cholerae* El Tor biofilm. Mol. Microbio. *34*, 586-595.

32. Yildiz, F.H., and Schoolnik, G.K. (1999). *Vibrio cholerae* O1 El Tor: Identification of a gene cluster required for the rugose colony type, exopolysaccharide production, chlorine resistance, and biofilm formation. Proc. Natl. Acad. Sci. U.S.A. *96*, 4028-4033.

33. Yildiz, F.H., and Visick, K.L. (2009). *Vibrio* biofilms: so much the same yet so different. Trends Microbiol *17*, 109-118.

34. Teschler, J.K., Zamorano-Sánchez, D., Utada, A.S., Warner, C.J.A., Wong, G.C.L., Linington, R.G., and Yildiz, F.H. (2015). Living in the matrix: assembly and control of *Vibrio cholerae* biofilms. Nat. Rev. Microbiol. *13*, 255-268.

35. Bilecen, K., and Yildiz, F.H. (2009). Identification of a calcium-controlled negative regulatory system affecting *Vibrio cholerae* biofilm formation. Environ. Microbiol. *11*, 2015-2029.

36. Wucher, B.R., Bartlett, T.M., Hoyos, M., Papenfort, K., Persat, A., and Nadell, C.D. (2019). *Vibrio cholerae* filamentation promotes chitin surface attachment at the expense of competition in biofilms. Proc. Natl. Acad. Sci. U.S.A. *116*, 14216-14221.

37. Tamayo, R., Patimalla, B., and Camilli, A. (2010). Growth in a biofilm induces a hyperinfectious phenotype in *Vibrio cholerae*. Infect. Immun. *78*, 3560-3569.

38. Meibom, K.L., Blokesch M, Dolganov NA, Wu C-Y, and GK, S. (2005). Chitin induces natural competence in *Vibrio cholerae*. Science *310*, 1824-1827.

Abbreviations: CBM, carbohydrate-binding module; GbpA, *N*-acetylglucosamine binding protein A; D-GbpA, deuterated GbpA; Electron Microscopy (EM); H-GbpA, hydrogenated (= non-deuterated) GbpA; HAc, acetic acid; ILL, Institut Laue Langevin; LPMO, lytic polysaccharide monooxygenase; NIST, National Institute of Standards and Technology; PDB, Protein Data Bank; SANS, Small-Angle Neutron Scattering; SAXS, Small-Angle X-ray Scattering; USANS, Transmission Electrom Microscopy (TEM); Ultra-Small-Angle Neutron Scattering.

Figures

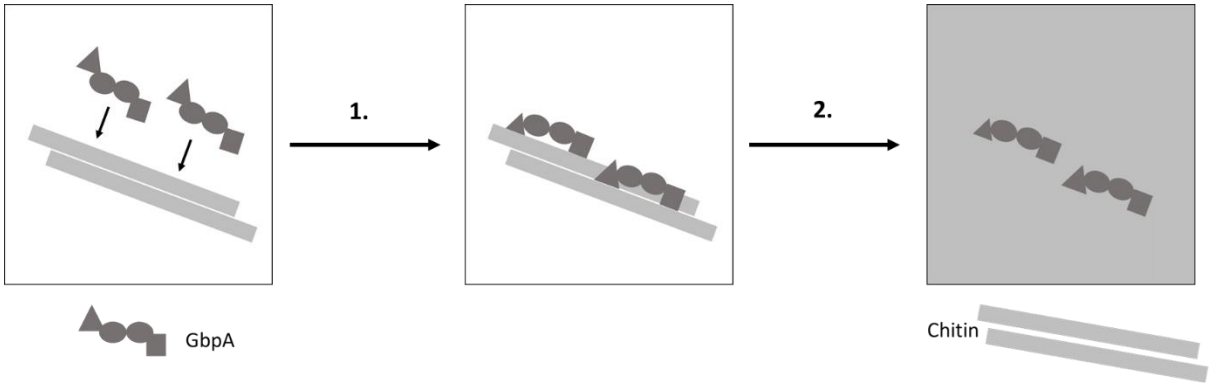

Figure 1 Schematic representation of the experiment 1. GbpA binds chitin, undergoing a conformational change. **2.** By applying mixtures of D_2O and H_2O using SANS, chitin can be matched out, leaving GbpA as the only visible scatterer.

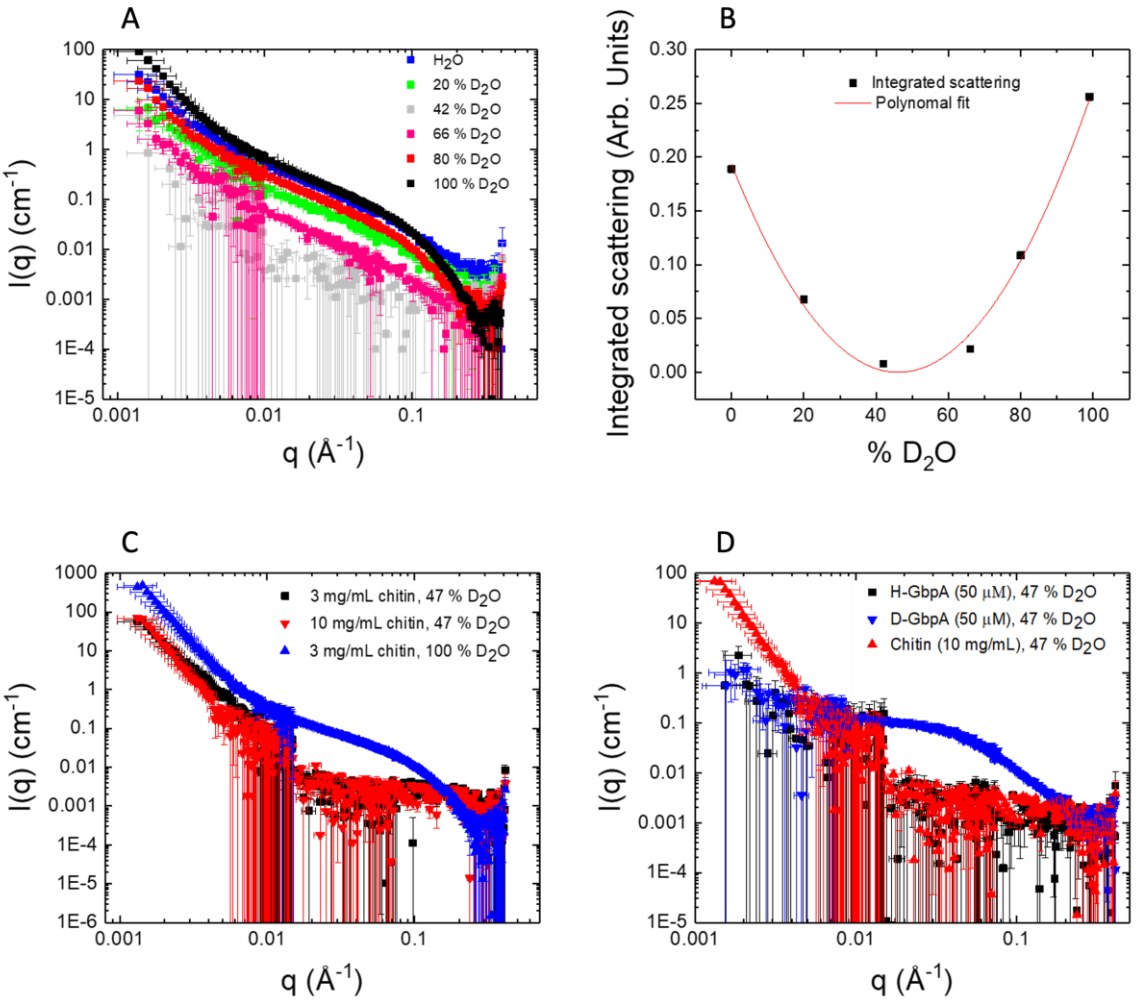

Figure 2 Matching out chitin in SANS experiments A 10 mg/mL chitin was subjected to SANS at six different ratios of D_2O to H_2O, and the data were plotted as intensities (I(q)) vs. the scattering vector (q) on double-logarithmic scale. **B** The scattering for each of the six conditions was integrated, plotted and fitted with a polynomial function, to find the chitin match point at minimal scattering intensity (determined to be at 47% D_2O). **C** The scattering of chitin in 47% D_2O is significantly weaker than in 100% D_2O, and is matched out in the middle to high q-range. However, at low-q, chitin could not be perfectly matched out. **D** In 47% D_2O, D-GbpA scatters well in the middle to high q-range, where both chitin and H-GbpA are well matched-out. Error bars represent one standard deviation.

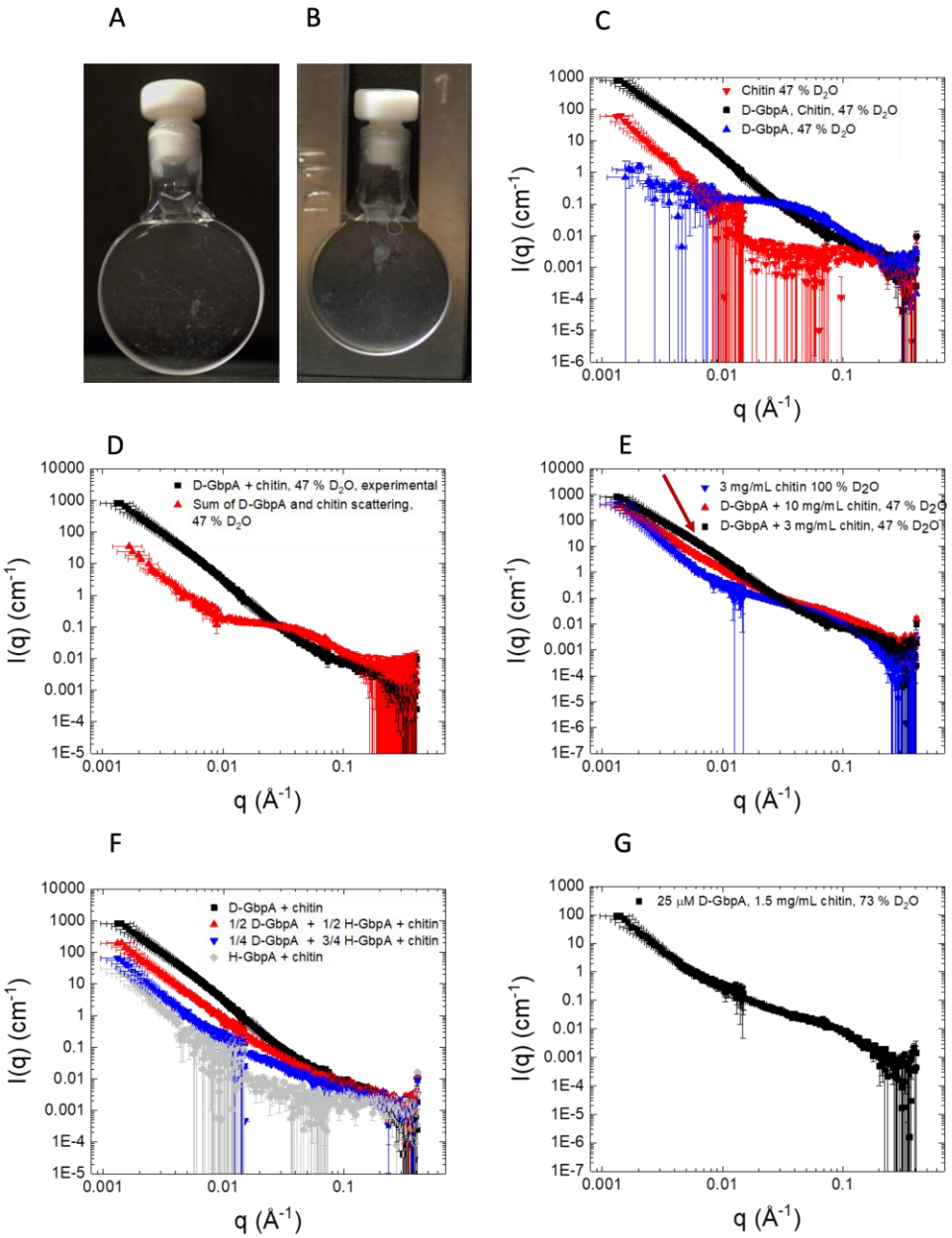

Figure 3 Sample preparation and SANS experiments A, B Images of 3 mg/mL chitin samples, without GbpA (A) or with 50 µM (2.5 mg/mL) GbpA (B). **C-G** SANS data of GbpA, chitin or GbpA-chitin mixtures, plotted as intensities (I(q)) vs. the scattering vector (q) on double-logarithmic scale. Unless stated otherwise, 3 mg/mL chitin (except samples of GbpA alone), 50 µM GbpA (combined concentration of H-GbpA and D-GbpA; except for samples of chitin alone) was used and measurements were done at 47% D_2O. **C, D** Chitin and D-GbpA clearly form a complex, since the SANS data of the mixture is significantly different from the sum of the scattering of the individual biomolecules. **E** Increasing the amount of chitin relative to GbpA changes the overall structure of the GbpA aggregate, but the steep slope at low-q persists, suggesting a structural correlation between the proteins. The bump at mid-q (indicated by red arrow), may be related to changes in fiber thickness upon GbpA binding. **F** Varying H-GbpA to D-GbpA ratios affected the structure factor (intensities were lower for higher fractions of H-GbpA, since H-GbpA is almost matched at 47% D_2O), but the steep slope at low-q persisted. **G** Measurement in the middle of the chitin and D-GbpA match point yielded a slope close to the average of the slope for chitin and the complex at 47% D_2O. Error bars represent one standard deviation.

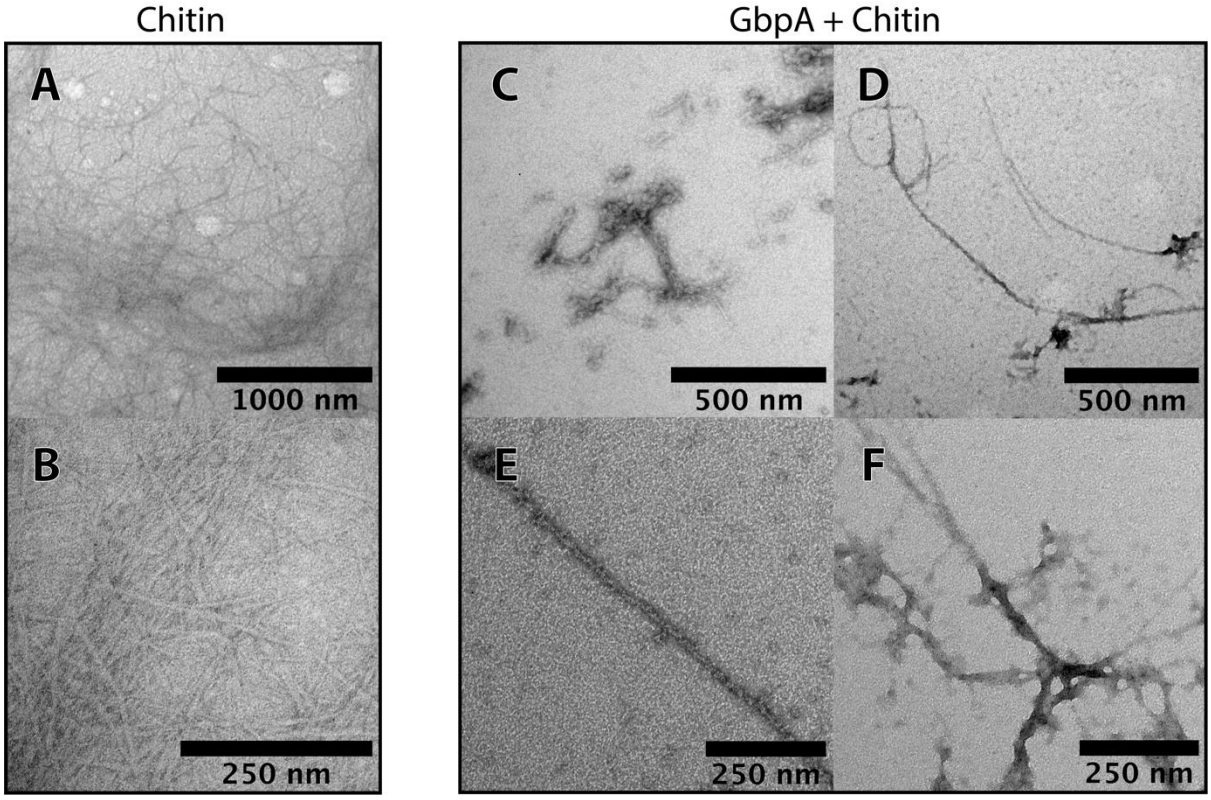

Figure 4 Negative-stain EM of chitin and GbpA A, B Examples of chitin images. Some fibers form bundles, but most of the chitin fibers are well separated after sonication. **C to F** Complex of chitin and GbpA. Individual chitin fibers appear to be coated with GbpA, as the fibers are thicker and more electron-dense (D and E) compared to chitin alone (A, B). In addition to protein-coated fibers, we observed aggregation between fibers in the presence of GbpA (C, D and F).

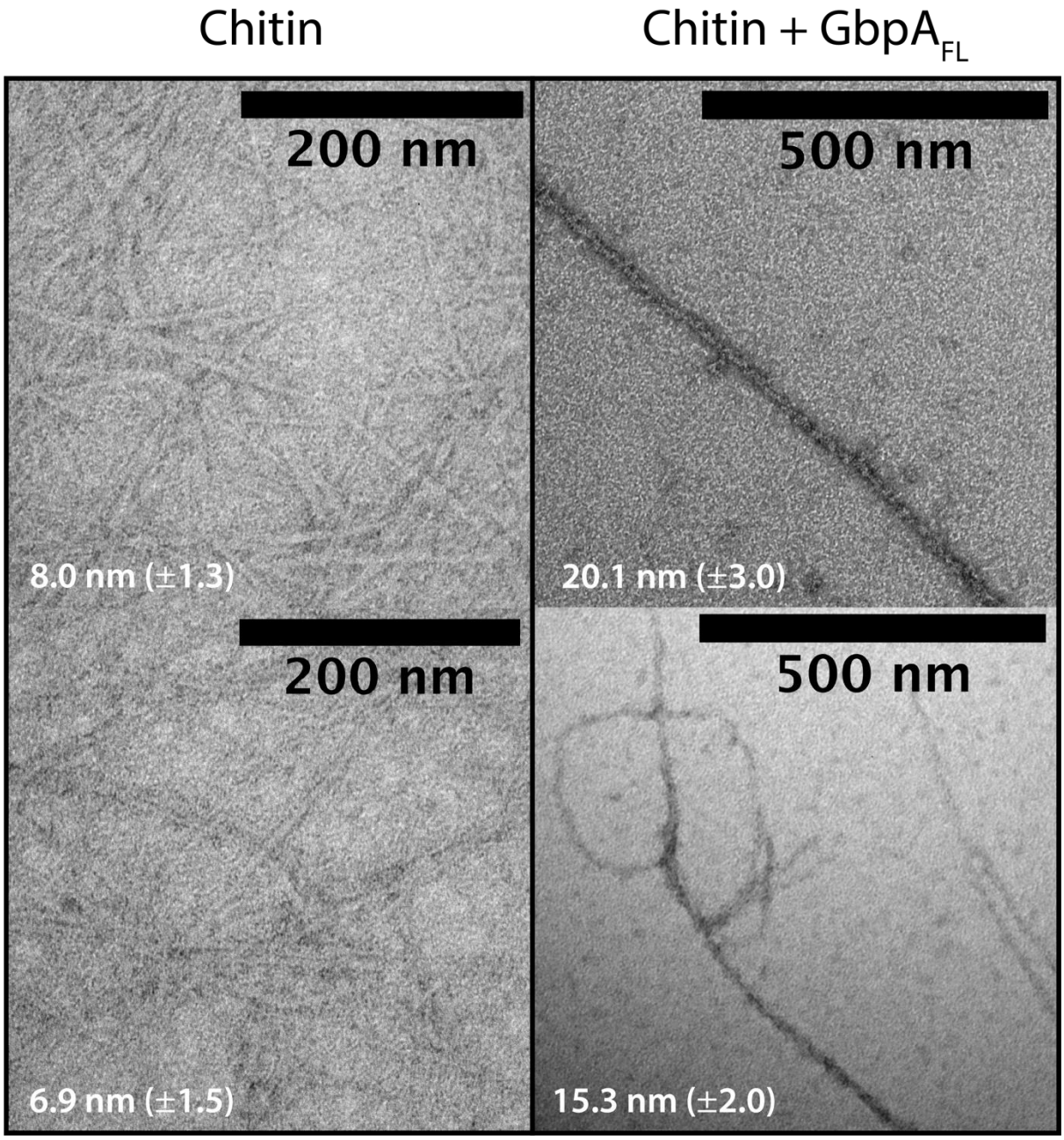

Figure 5 Measurement of chitin fiber thickness. Fibres were measured in micrographs of chitin, alone and in the presence of GbpA. The average thickness of fibres in each micrograph is shown at the bottom left. Standard deviations are given in parentheses. 15 measurements were performed for each micrograph, using Image J.

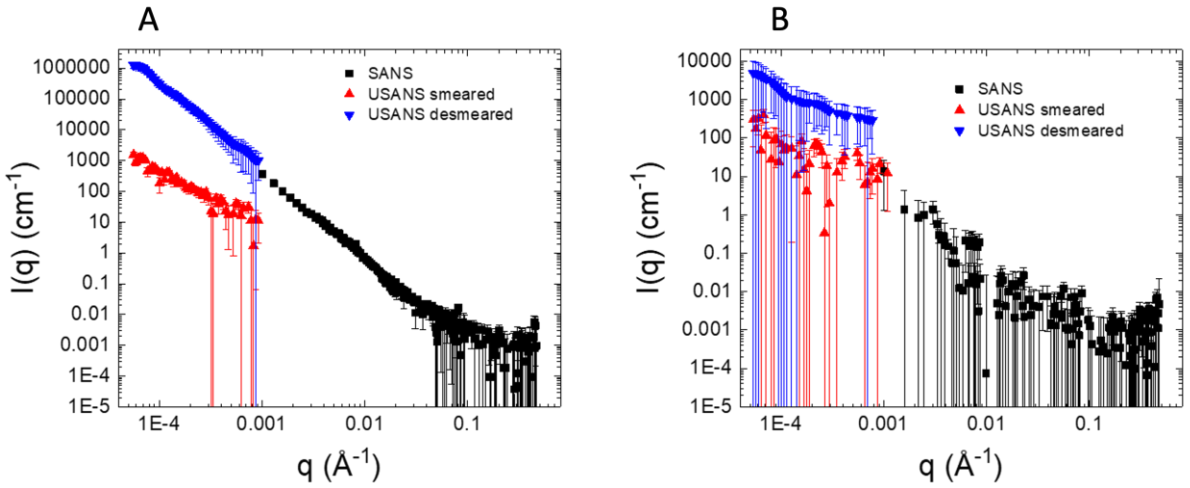

Figure 6 SANS and USANS data A GbpA bound to chitin and **B** Chitin alone. Data were collected at 47% D_2O. USANS data confirmed a structural order in the micrometer regime. Error bars represent one standard deviation.

Tables

Table 1: Fitting parameters

Sample	Fitting range ($Å^{-1}$)	Decay exponent	Scaling factor	R^2
Chitin (3 mg/mL) (100% D_2O)	0.0015-0.005	4.3	3.1×10^{-10}	0.999
D-GbpA (50 µM) + Chitin (3 mg/mL)	0.0015-0.005	2.7	1.4×10^{-5}	0.999
D-GbpA (50 µM) + Chitin (10 mg/mL)	0.0016-0.005	3.0	1.3×10^{-5}	0.999
D-GbpA (25 µM) + H-GbpA (25 µM) + Chitin (3 mg/mL)	0.0014-0.005	2.8	4.1×10^{-7}	0.996
D-GbpA (12.5 µM) + H-GbpA (37.5 µM) + Chitin (3 mg/mL)	0.0014-0.004	3.5	5.2×10^{-9}	0.996
H-GbpA (50 µM) + Chitin (3 mg/mL)	0.0015-0.005	3.7	8.4×10^{-10}	0.997
D-GbpA (25 µM) + Chitin (1.5 mg/mL) (73.5% D_2O)	0.0015-0.005	3.4	1.4×10^{-8}	0.997

Samples in 47% D_2O unless else is stated